

Entry of Epidemic Keratoconjunctivitis-Associated Human Adenovirus Type 37 in Human Corneal Epithelial Cells

Ji Sun Lee, Santanu Mukherjee, Jeong Yoon Lee, Amrita Saha, James Chodosh, David F. Painter, and Jaya Rajaiya

Howe Laboratory, Massachusetts Eye and Ear, Department of Ophthalmology, Harvard Medical School, Boston, Massachusetts, United States

Correspondence: Jaya Rajaiya, Massachusetts Eye and Ear, 243 Charles Street, Boston, MA 02114, USA; jaya_rajaiya@meei.harvard.edu.

Received: May 15, 2020

Accepted: July 27, 2020

Published: August 27, 2020

Citation: Lee JS, Mukherjee S, Lee JY, et al. Entry of epidemic keratoconjunctivitis-associated human adenovirus type 37 in human corneal epithelial cells. *Invest Ophthalmol Vis Sci.* 2020;61(10):50. <https://doi.org/10.1167/iovs.61.10.50>

PURPOSE. Ocular infection by human adenovirus species D type 37 (HAdV-D37) causes epidemic keratoconjunctivitis, a severe, hyperacute condition. The corneal component of epidemic keratoconjunctivitis begins upon infection of corneal epithelium, and the mechanism of viral entry dictates subsequent proinflammatory gene expression. Therefore, it is important to understand the specific pathways of adenoviral entry in these cells.

METHODS. Transmission electron microscopy of primary and tert-immortalized human corneal epithelial cells infected with HAdV-D37 was performed to identify the means of viral entry. Confocal microscopy was used to determine intracellular trafficking. The results of targeted small interfering RNA and specific chemical inhibitors were analyzed by quantitative PCR, and Western blot.

RESULTS. By transmission electron microscopy, HAdV-D37 was seen to enter by both clathrin-coated pits and macropinocytosis; however, entry was both pH and dynamin 2 independent. Small interfering RNA against clathrin, AP2A1, and lysosome-associated membrane protein 1, but not early endosome antigen 1, decreased early viral gene expression. Ethyl-isopropyl amiloride, which blocks micropinocytosis, did not affect HAdV-D37 entry, but IPA, an inhibitor of p21-activated kinase, and important to actin polymerization, decreased viral entry in a dose-dependent manner.

CONCLUSIONS. HAdV-D37 enters human corneal epithelial cells by a noncanonical clathrin-mediated pathway involving lysosome-associated membrane protein 1 and PAK1, independent of pH, dynamin, and early endosome antigen 1. We showed earlier that HAdV-D37 enters human keratocytes through caveolae. Therefore, epidemic keratoconjunctivitis-associated viruses enter different corneal cell types via disparate pathways, which could account for a relative paucity of proinflammatory gene expression upon infection of corneal epithelial cells compared with keratocytes, as seen in prior studies.

Keywords: adaptor protein, adenovirus, clathrin mediated endocytosis, dynamin, epidemic keratoconjunctivitis, epithelial cells, macropinocytosis, trafficking, viral entry

Human adenoviruses (HAdV) are members of the family Adenoviridae, genus *Mastadenovirus*, that cause infections of respiratory, gastrointestinal, genitourinary, and ocular surface mucosa in both immunocompromised and immunocompetent hosts.¹ To date, there are more than 100 distinct HAdV genotypes divided into seven species (A–G).² Human adenovirus species D (HAdV-D) is the largest HAdV species, and includes the types most commonly responsible for epidemic keratoconjunctivitis (EKC), the most severe form of ocular surface infection. Studies from our laboratory and others have identified new eye pathogens, including types D53, D54, and D56, in addition to the more common ones D8, D37, and D64, which cause EKC.^{3–5} To date, no specific treatment is available for adenoviral corneal infections. Therefore, a detailed understanding of viral entry and trafficking are paramount to design new therapies.⁶ Although the means of viral entry for HAdV species C have

been studied in detail,^{7–10} the biology of HAdV-D infection of ocular surface epithelial cells remains relatively underexplored.

The primary interaction of adenovirus with its cellular target occurs between the adenoviral fiber knob and a range of host cell surface receptors, including CD46, Coxsackievirus adenovirus receptor, and GD1a glycan.^{11–15} Recent data showing that HAdV-D associated with EKC bind to GD1a glycan to infect human corneal epithelium have been exploited with therapeutic potential.^{6,13–16} After fiber knob binding, a secondary attachment between arginine–glycine–aspartic acid motifs on the capsid penton base protein with cell surface integrins leads to a cell signaling cascade that initiates viral entry.^{17–19}

Viruses use several mechanisms to enter host cells, including clathrin-mediated endocytosis, macropinocytosis, and caveolin-mediated endocytosis. Clathrin-mediated

endocytosis is the best characterized and the paradigm viral entry pathway.²⁰ Studies using biochemical inhibitors and dominant-negative mutants demonstrated that entry of HAdV-C2 and -C5 are clathrin dependent,^{21,22} although other reports using different cell types suggest macropinocytosis as an alternate entry pathway.²³ For other adenoviruses, for example, HAdV-B3, macropinocytosis is the primary entry pathway.²⁴ In part because the protein machinery that mediates endocytosis differs by endocytotic pathway, it is postulated that the physical process of viral entry is directly associated with subsequent intracellular trafficking.^{25–27} However, considerable plasticity exists such that certain components, such as dynamin 2, Rho GTPases, and actin, can participate in more than one endocytotic pathway. We recently showed that the EKC pathogen HAdV species D type 37 (HAdV-D37) enters human keratocytes through caveolae, in a caveolin 1-dependent manner.²⁵ It is becoming more apparent that the entry pathway(s) used by the virus may be cell and virus type specific.

In this study, we use biochemical and molecular approaches to elucidate entry and trafficking of HAdV-D37 in both primary and immortalized human corneal epithelial cells. Electron microscopy was applied to analyze viral entry and visualize the intracellular positioning of HAdV-D37 virions. We then systematically inhibited the function of key cellular factors involved in the various endocytic pathways. Our findings indicate that HAdV-D37 cellular entry occurs primarily by clathrin-mediated endocytosis, but in a dynamin-independent manner. Further, we found HAdV-D37 entry is dependent on modification of actin, but does not require key components of canonical clathrin-mediated endocytosis, such as epsin, endosomal acidification, or early endosome antigen 1 (EEA1).

METHODS

Cells and Virus

Primary human corneal epithelial (PHCE) cells were isolated from donor corneal tissue following a published protocol²⁸ and pooled. Briefly, the cornea was treated with dispase solution containing 20 µg/mL gentamycin in Hanks balanced salt solution and incubated for 24 hours at 4°C. The epithelial layer was then gently scraped into the media, and treated with 0.25% trypsin to prepare a single cell suspension. The cells were plated and grown in Defined Keratinocyte-SFM (1×) basal media with 0.2% growth supplement (Thermo Fisher Scientific, Waltham, MA) and a 1% penicillin-streptomycin solution (Thermo Fisher Scientific). Primary cells were used at the second passage.

Tert-immortalized human corneal epithelial (THE) cells were the kind gift of Jerry Shay (University of Texas Southwestern Medical Center). THE cells were grown in Defined Keratinocyte-SFM (1×) media as described above. HAdV-D37, originally isolated from 62 eyes and 9 genitourinary sites,²⁹ and later whole genome sequenced (Gen Access no: DQ900900),³⁰ was obtained from the American Type Culture Collection (Manassas, VA) and grown in A549, human lung carcinoma cells (American Type Culture Collection) in Dulbecco's Modified Eagle Medium with 2% fetal bovine serum (FBS), and 1% penicillin streptomycin solution (all from Thermo Fisher Scientific). Virus was purified from A549 cells after 7 days of infection using CsCl gradient ultracentrifugation, and subsequently dialyzed against a 10 mM Tris (pH 8.0) buffer containing 80 mM

NaCl, 2 mM MgCl₂, and 10% glycerol. Purified virus was titered in triplicate, and stored at -80°C. Cy3 labeling of HAdV-D37 was performed for select experiments as described elsewhere.³¹

Antibodies and Reagents

Antibody against cytokeratin 3/12 was purchased from Abcam (Cambridge, MA). Anti-acetylated tubulin (0.05 µg/mL), and chemicals including cytochalasin D, cytochalasin B, bafilomycin A1, 5-(N-ethyl-N-isopropyl)-Amiloride (EIPA), and IPA-3 were purchased from Sigma-Aldrich. Antibodies to clathrin and dynamin 2 were obtained from Abcam. Anti-adaptor protein 2 subunit alpha 1 (AP2A1) antibody and Transferrin-Alexa Fluor 568 were obtained from Thermo Fisher Scientific. Antibodies to glyceraldehyde-3-phosphate dehydrogenase (GAPDH), EEA1, and lysosome-associated membrane protein 1 (LAMP1) were obtained from Santa Cruz Biotechnology (Dallas, TX). Cy3 dye was obtained from GE Healthcare Life Sciences (Pittsburgh, PA). Lipofectamine RNAiMAX was obtained from Thermo Fisher Scientific.

Transmission Electron Microscopy

PHCE and THE cells grown to 95% confluence in 12-well plates were infected with HAdV-D37 virus at a multiplicity of infection of 100, incubated for 30 minutes at 4°C, and then 37°C for 30 minutes, 1 hour, or 2 hours, washed with PBS, fixed in 2% paraformaldehyde containing 2.5% glutaraldehyde, 0.1 M cacodylate and 2.5 mM CaCl₂ for 1 hour, and then harvested in 2% agarose. The washed cell pellet was fixed in 2% aqueous OsO₄, and dehydrated for 90 minutes. The cell pellet was subsequently embedded in epon and sectioned at 70 to 90 nm. The sections were stained with saturated aqueous uranyl acetate, and Sato's lead stain. Electron micrographs were captured on a Philips CM-10 electron microscope (Koninklijke Philips Electronics N.V., Amsterdam, the Netherlands) fitted with a CCD camera.

Real-Time PCR

To quantify viral entry, the HAdV-D37 E1A gene was amplified after selected time points of infection using primers (Integrated DNA Technologies [IDT], Coralville, IA, [Table](#)) designed based on the HAdV-D37 E1A nucleotide sequence.²⁶ Quantitative real-time PCR (RT-qPCR) was performed using Fast SYBR Green master mix (Applied Biosystems, Foster City, CA) with the following conditions: 40 cycles at 95°C (10 seconds), 60°C (1 minute), and 72°C (30 seconds), then a final extension at 72°C for 10 minutes. For chemical pretreatments, cells were exposed to specific inhibitors for indicated time periods followed by viral infection. E1A gene expression was then measured using RT-qPCR. To determine mRNA expression for clathrin, dynamin 2, AP2A1, epsin 1, EEA1, and LAMP1, total RNA was extracted from THE cells transfected with experimental small interfering RNA (siRNA) or control scrambled RNA (scRNA), at 2 hours post infection (hpi) using TRIzol Reagent (Invitrogen, Carlsbad, CA) according to the manufacturer's instructions. Total RNA was then treated with DNase I (1 unit) (New England BioLabs, Ipswich, MA) at 37°C for 1 hour followed by 20 minutes at 80°C to inactivate the DNase I. To obtain cDNA, 2 µg of the DNase-treated RNA was subjected to reverse transcription with M-MLV reverse transcriptase

TABLE. RT-qPCR Primers and siRNA Sequences

Primers and Sequences	Forward	Reverse
RT-qPCR		
E1A	ATG AGT CAT CAC CCT CAG AAG AAA	ACC CAT GTC ATG TAA CAA GTC CTC
Clathrin	AAC GTT GCA ATG AAC CTG CGG TCT GG	GAG CCT TCT TAC GGG CCA TCT GCA AG
DNM2	TGG ACA GCT GGA AGG CCT CGT TCC T	CCA GGT TGC GAA TGG TCT CCA
AP2A1	CTG CTT GGC ATT GCT CCG GTC ACA CA	TGG CCA GCT CCG AGT TCT CCC ATG AA
Epsin1	TCT GAC TTT GAC CGA CTC CGC ACG GC	CTG CCC ACA GCC TCA GCC AGA GAT
EEA1	ACA TGC ATC ACA GAC ACG AAC AGG CT	AAA CTG TAT GGC CTG TGG GAA AGG CT
LAMP1	GGC AAT TCC TAC AAG TGC AAC GCG GA	TGT TCT CGT CCA GCA GAC ACT CCT CC
Cav1	AGG CCA GCT TCA CCA CCT TC	GCC CAG ATG TGC AGG AAA GA
GAPDH	ATG CCT CCT GCA CCA CCA ACT GCT TA	GTG GCA GTG ATG GCA TGG ACT GTG GT
siRNA		
	Sense Sequences	Antisense Sequences
Clathrin siRNA 1	rGrCrA rArArU rUrArC rCrUrA rArCrA rUrArA rGrCrU rCrCA C	rGrUrG rGrArG rCrUrU rArUrG rUrUrA rGrGrU rArArU rUrUrG rCrCrU
Clathrin siRNA 2	rGrGrC rUrUrC rUrArA rArUrA rUrGrA rArCrAxbrk rArCT G	rCrArG rUrUrG rUrUrC rArUrG rArUrA rUrUrU rArGrA rArGrC rCrArC
Clathrin siRNA 3	rGrCrC rUrUrU rArCrA rArGrG rArUrG rCrArA rUrGrC rArGT A	rUrArC rUrGrC rArUrU rGrCrA rUrCrC rUrUrG rUrArA rArGrG rCrUrG
DNM2 siRNA-1	rGrCrA rGrUrC rCrUrA rCrArU rCrArA rCrArC rGrArA rCrCA T	rArUrG rGrUrU rCrGrU rGrUrU rGrArU rGrUrA rGrGrA rCrUrG rCrUrC
DNM2 siRNA-2	rArGrU rUrUrG rArCrC rArCrU rGrUrA rArGrU rGrCrC rUrGC A	rUrGrC rArGrG rCrArC rUrUrA rCrArG rUrGrG rUrCrA rArArC rUrGrA
DNM2 siRNA-3	rCrGrC rCrArC rArCrG rUrGrU rUrGrA rArCrU rUrGrA rCrCC T	rArGrG rGrUrC rArArG rUrUrC rArArC rArCrG rUrGrU rGrGrC rGrArG
AP2A1_SEQ1	rGrCrC rUrUrG rGrArU rGrGrC rUrArC rArGrU rArArG rArAA A	rUrUrU rUrCrU rUrArC rUrGrU rArGrC rCrArU rCrCrA rArGrG rCrUrU
AP2A1_SEQ2	rGrGrU rGrCrA rUrUrC rCrArA rCrGrC rCrArA rGrAA C	rGrUrU rCrUrU rGrGrC rGrUrU rGrGrA rArUrG rCrUrG rCrArC rCrUrU
AP2A1_SEQ3	rCrGrC rArGrA rArGrU rUrArC rUrArA rGrGrC rCrArA rGrCT T	rArArG rCrUrU rGrGrC rCrUrU rArGrU rArArC rUrUrC rUrGrC rGrUrC
LAMP1.		

(Promega, Madison, WI) and anchored oligo(dT)15primers (IDT). All primers were designed using Primer3 plus software (<http://www.bioinformatics.nl/cgi-bin/primer3plus/primer3plus.cgi>), and synthesized by IDT (Table). The resulting cDNAs were diluted 10 fold, and 1 μ L of diluted cDNA was used for RT-qPCR using Fast SYBR Green master mix under the following conditions: 40 cycles at 95°C (30 seconds), 60°C (1 minute), 72°C (30 seconds), and a final extension at 72°C for 10 minutes. A no template control and an endogenous control (GAPDH) were measured, and the expression levels were calculated by the $2^{-\Delta\Delta CT}$ method and compared with the scRNA and mock-infected controls.

Confocal Microscopy

Cells grown on chamber slides (Thermo Fisher Scientific) were treated with specific siRNA or scRNA controls for 48 hours, and then infected with Cy3-labeled HAdV-D37 for 2 hours. Cells were then partially fixed in 0.05% paraformaldehyde for 10 minutes, washed in PBS containing 2% BSA, and permeabilized for 5 minutes in solution containing 0.1% Triton X-100 for 5 minutes. After 30 minutes blocking in 3% FBS-PBS, the cells were incubated in 5 μ g/mL of Alexa Fluor 488 phalloidin (Thermo Fisher Scientific) for 30 minutes at room temperature, and washed three times in 1 \times PBS containing 2% FBS. Antibodies to cytokeratin3/12 (1 μ /mL), clathrin (1:1000, Abcam), and acetylated tubu-

lin (1:1000, Sigma-Aldrich) were incubated for 1 hour at room temperature, followed by three washes in 1 \times PBS containing 2% FBS. Cells were then incubated with Alexa Fluor 488 conjugated secondary antibody (1:1000, Thermo Fisher Scientific) for 45 minutes at room temperature. For colocalization studies, cells were infected with Cy3-labelled virus for 30 minutes on ice, further incubated for 1 hour at 37°C, and then washed in PBS, followed by transferrin (Alexa Fluor 568 or 488) treatment for 30 minutes. Cells were washed and mounted using VECTASHIELD mounting medium (Vector Laboratories, Burlingame, CA) containing DAPI. Images were captured with a Leica SP5 confocal microscope using a 63 \times oil immersion objective. Images were scanned at 0.5 μ m intervals, to obtain 15 to 20 Z-stacks each, then constructed by maximum projection.

siRNA Transfection

Transfections were carried out using Lipofectamine RNAiMAX reagent (Thermo Fisher Scientific), following the manufacturer's protocol. A maximum of three target siRNAs per gene were made to order by IDT. Pooled scRNA was directly purchased from Ambion as indicated (Table). We mixed 100 pmol of siRNA or scRNA in 500 μ L of Opti-MEM I Reduced Serum Medium (Thermo Fisher Scientific), followed by the addition of 5 μ L of Lipofectamine RNAiMAX. After 20 minutes incubation at room temperature, the transfection complex was added to cells

at 60% to 80% confluence. After 48 hours transfection, THE cells were infected with HAdV-D37 at an multiplicity of infection of 10 for 30 minutes on ice. Cells were washed to remove unbound viruses, and further incubated at 37°C for 1 or 2 hours for virus internalization. The cells were then processed for confocal microscopy, Western blot, or RT-qPCR analysis.

Western blot

For Western blot, HAdV-D37 and mock-infected cells were lysed with chilled cell lysis buffer (20 mM Tris, pH 7.4, 150 mM NaCl, 1 mM EDTA, 1 mM EGTA, 1% Triton X-100, 2.5 mM sodium pyrophosphate, 1 mM β -glycerol phosphate, 1 mM Na_3VO_4 , 1 $\mu\text{g}/\text{mL}$ leupeptin, and 1 mM PMSF) (Cell Signaling Technology, Danvers, MA) and incubated at 4°C for 5 minutes. The cell lysates were cleared by centrifugation at 14,000 \times g for 10 minutes. The protein concentration of each supernatant was measured by BCA analysis (Pierce, Rockford, IL) and equalized. Twenty micrograms of cell lysate was subsequently separated by 10% SDS-PAGE and transferred onto nitrocellulose membranes (Bio-Rad Laboratories, Hercules, CA). The protein bands were visualized with Super Signal West Dura Extended Duration Substrate (Thermo Fisher Scientific).

Statistical Analysis

Each experiment was performed at least three times, except for the transmission electron microscopy, which was performed twice. Quantitative data was analyzed by Student *t*-test or ANOVA with Tukey's multiple comparisons test using GraphPad Prism (San Diego, CA). Statistical significance was reported for a *P* value equal to or less than 0.05 (denoted by *).

RESULTS

Ultrastructure of Adenovirus Entry Into Human Corneal Epithelial Cells

Viruses are known to use multiple and often redundant pathways to enter cells that allow them to overcome cell barriers to entry.^{32,33} To characterize the entry pathways for HAdV-D37 in human corneal epithelial cells, we used both PHCE and THE cells, the latter immortalized with a retroviral vector encoding human telomerase reverse transcriptase but retaining expression of the corneal epithelial marker cytokeratin 3.³⁴ We earlier showed that HAdV-D37 uses caveolae for entry into human keratocytes.²⁵ By TEM performed on HAdV-D37-infected PHCE and THE cells, at 15 minutes post incubation at 37°C, we found electron dense virions within both clathrin-coated pits (Fig. 1B, 1H) and at membrane ruffles (Fig. 1E, 1K), suggesting that both clathrin-mediated endocytosis and macropinocytosis as active entry pathways. By 30 minutes and 1 hpi (Figs. 1C, 1F, 1I, 1L, and Figs. 1D, 1G, 1J, 1M), respectively, virions were seen within endosomes and vesicles containing multivesicular bodies. The latter serve as endosomal maturation pathways, that can lead to either productive intracellular trafficking or lysosomal degradation and autophagy. Multivesicular bodies also serve as signalosomes (foci) of intracellular signaling.³⁵⁻³⁷

Clathrin-Dependent Entry of Adenovirus

Adenovirus has previously been shown to use clathrin-mediated entry across many cell types.³⁸⁻⁴⁰ However, most such studies used either HAdV-C2 or -C5, which are not corneal pathogens. We earlier showed that HAdV-C2 does not enter corneal fibroblasts, indicating cell specific tropism.²⁵ Because the TEM results were suggestive of viral entry by a clathrin mediated pathway in both PHCE and THE cells, we used THE cells to further confirm the role of clathrin. Confocal microscopy of THE cells at 2 hpi Cy3-labeled HAdV-D37 showed intracellular Cy3 label (Fig. 2A), indicating successful viral entry. As predicted based on the TEM data, siRNA knockdown of clathrin, as confirmed by Western blot and RT-qPCR (Fig. 2B), decreased the Cy3 signal. E1A gene expression, which was measured as a surrogate marker for viral entry, was also reduced significantly ($P \leq 0.05$) in cells pretreated with siRNA against clathrin as compared with scRNA treated cells (Fig. 2B). Co-localization (yellow) of clathrin (green) and Cy3-labelled HAdV-D37 (red) was confirmed by confocal microscopy performed at 1 hpi (Fig. 2C, upper row). The internalization of transferrin is often used to confirm a functional, clathrin-mediated entry pathway in cells.⁴¹⁻⁴³ Co-localization between transferrin (green) and Cy3-labeled HAdV-D37 (red) was also observed (Fig. 2C, middle row), as was co-localization between clathrin (green) and transferrin (red) (Fig. 2C, lower row). These results strongly indicate clathrin-mediated entry for HAdV-D37 into THE cells.

Dynamin 2-Independent Entry of Adenovirus

Dynamin 2 is a large GTPase, originally identified as a microtubule binding protein, and its mutations cause neurologic disorders, such as Charcot-Marie-Tooth disease.⁴⁴ Some viruses have been shown to enter in a dynamin 2-dependent manner.^{45,46} In contrast, our recent study of HAdV-D37 entry into human keratocytes demonstrated a negative role for dynamin 2 in viral entry. Dynamin 2 knock down in keratocytes increases acetylation of tubulin, and localizes microtubule organizing centers closer to the nuclear membrane, enabling increased nuclear entry of viral DNA.²⁶ However, in THE cells knocked down for dynamin 2 by siRNA, we observed no change in acetylated tubulin or viral entry as compared with scRNA-treated control cells (Fig. 3A). Similarly, we found no change in HAdV-D37 E1A gene expression (Fig. 3B). Knock down of dynamin 2 is shown by Western blot and RT-qPCR (Fig. 3B). These results suggest that in THE cells, HAdV-D37 entry is dynamin 2 independent.

Role of Adapter Protein 2 in Entry of Adenovirus

Key molecules important to the canonical clathrin-mediated endocytosis pathway include actin, epsin, epidermal growth factor receptor pathway substrate clone 15, adaptor protein 2 (AP2), phospholipid phosphatidylinositol 4,5-bisphosphate [PI(4,5)P₂], and PI(3,4,5)P₃. AP2 is generally considered to be critical to clathrin mediated endocytosis, although AP2-independent endocytosis has been observed.⁴⁷⁻⁵⁰ Upon siRNA-mediated knock down of AP2A1, as shown by Western blot and RT-qPCR (Fig. 4B) we observed abrogation of HAdV-D37 entry by confocal microscopy (Fig. 4A), and E1A gene expression (Fig. 4B) ($P \leq 0.05$). In contrast, siRNA knockdown of epsin 1, a secondary adapter protein

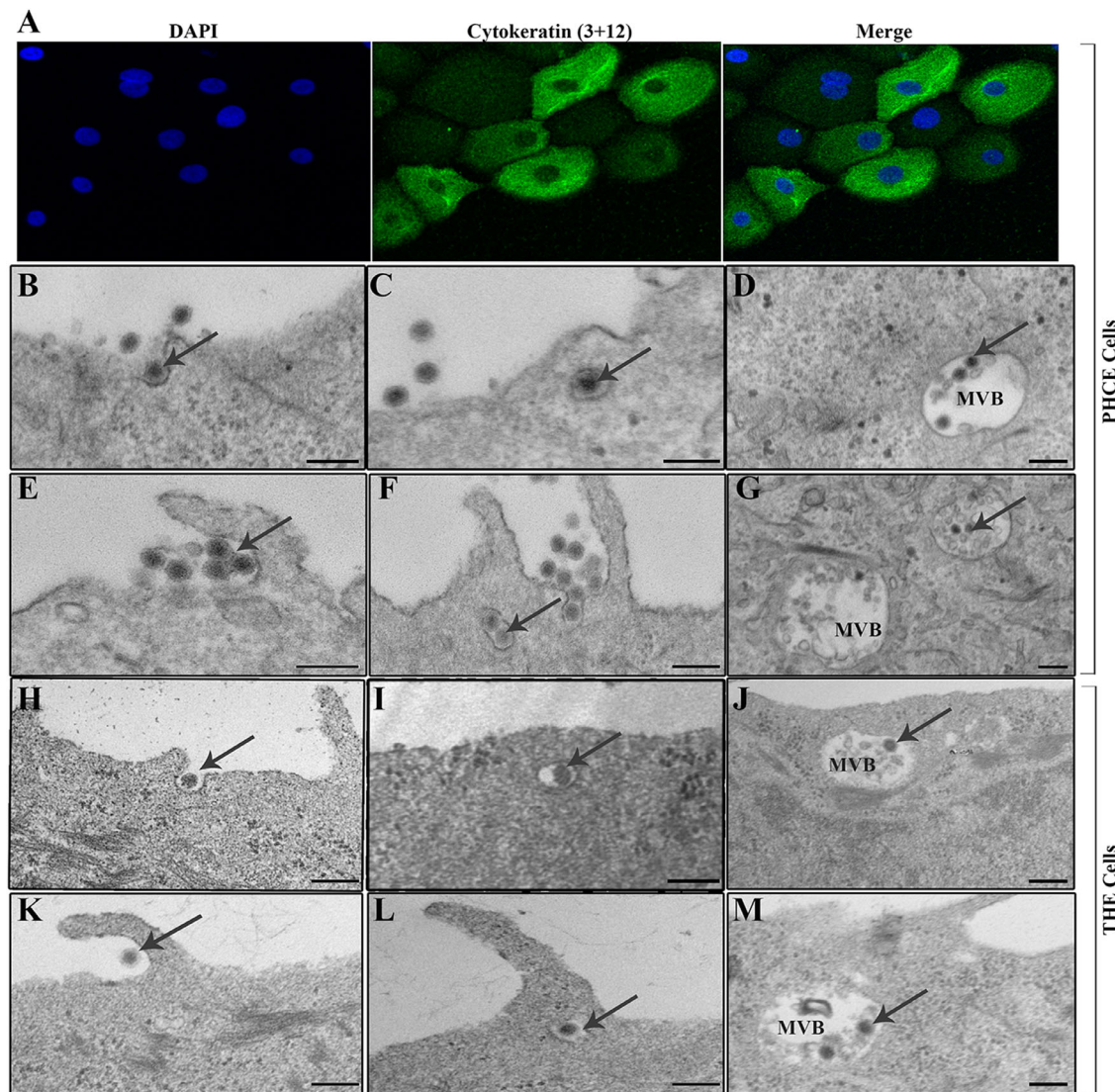


FIGURE 1. Transmission electron microscopy of HAdV-D37-infected PHCE (A–G) and THE cells (H–M). (A) PHCE expression of cytokeratin marker 3/12 was performed to confirm a corneal epithelial phenotype. DAPI staining was included to show cell nuclei. In representative images from 15 minutes post infection, PHCE cells show a virion (arrow) (B and H) within a clathrin pit like structure, and viruses within a membrane ruffle (E and K), suggesting uptake by macropinocytosis. By 30 minutes hpi (C, F, I, and L), virions can be seen in individual intracellular endosomes in both PHCE and THE cells, and by 1 hpi (D, G, J, and M) within vesicles containing multivesicular bodies (MVB). Scale bar = 200 microns.

previously shown to be important in maturation of clathrin coated pits,⁵¹ and in the internalization of influenza virus,⁵² had no apparent effect on E1A expression (Fig. 4C).

EEA1 Is Dispensable in Adenovirus Entry

EEA1 and LAMP1 are markers for early and late endosomes, respectively. EEA1 is a Rab5 effector and plays an important role in endosome fusion by tethering clathrin-coated vesicles to early endosomes.⁵³ However, one study implied that depletion of cytosolic EEA1 only partially inhibited endosome fusion, and that the residual EEA1 bound to endosome membranes might still aid in the fusion process.⁵⁴ In THE cells, knockdown of LAMP1 but not EEA1 reduced E1A expression at 2 hpi (Figs. 5A, 5B) ($P \leq 0.05$). These data suggest that EEA1 might be dispensable for HAdV-D37 entry, although trafficking

through late endosomes is required for early adenovirus gene expression.

Actin-Dependent, pH-Independent Adenovirus Entry

Actin is consistently engaged upon a cell's interaction with external particles, including viruses,⁵⁵ and in turn viruses have evolved to manipulate the actin cytoskeleton in all phases of infection.⁵⁶ Actin polymerization is an indispensable event in all endocytosis paradigms,⁵⁷ including macropinocytosis, phagocytosis, and both clathrin-dependent and -independent endocytotic pathways. During endocytosis, actin mediates the crucial formation of filopodia and/or microvilli. The chemical agents cytochalasin D and B inhibit actin polymerization, and actin network

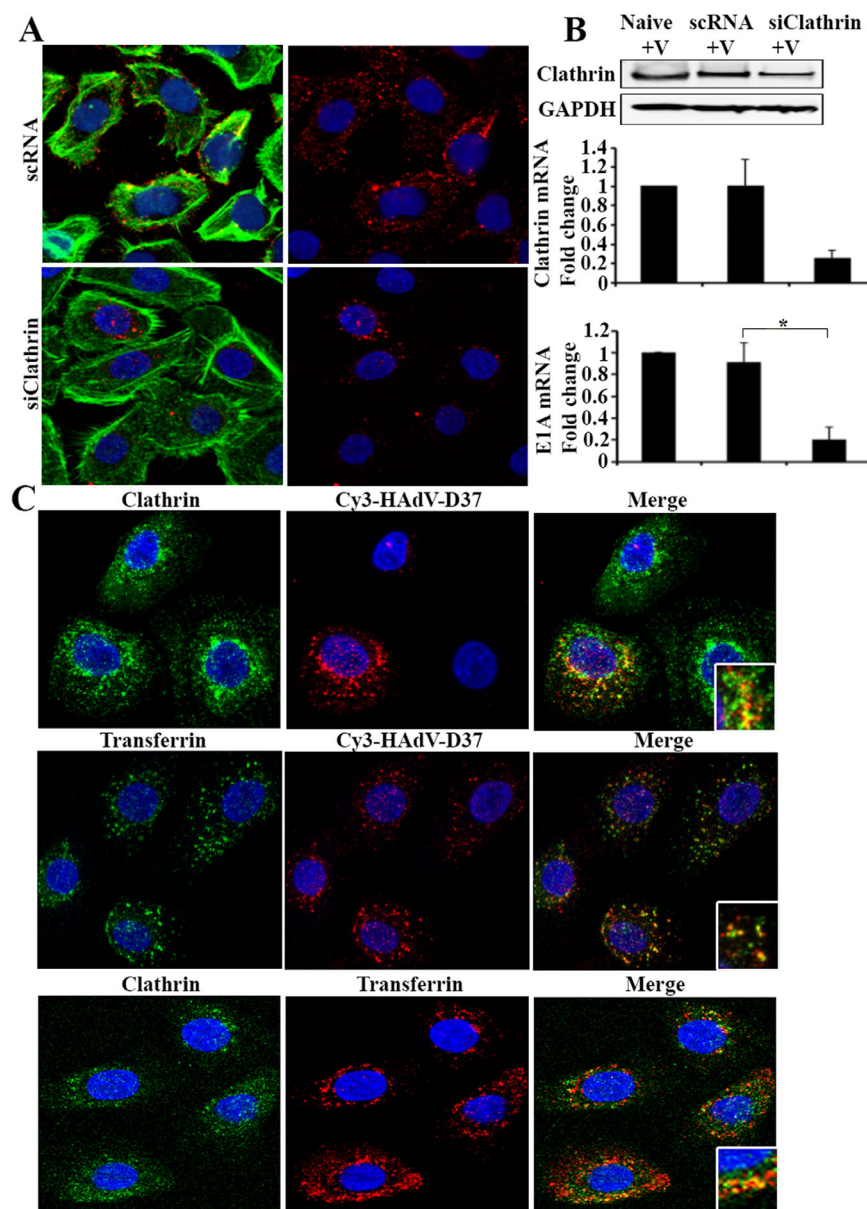


FIGURE 2. HAdV-D37 enters THE cells via a clathrin mediated pathway. **(A)** Confocal microscopy of THE cells pretreated with scRNA (*top*) or siClathrin (*bottom*) show a reduction in Cy3 labelled HAdV-D37 (*red*) in siClathrin treated cells at 2 hpi. Phalloidin staining is shown in green. **(B)** Clathrin knockdown, as shown by Western blotting and mRNA expression via RT-qPCR quantification. Reduced E1A gene expression is evident by RT-qPCR in clathrin knock down cells ($P \leq 0.05$). **(C)** Confirmation of clathrin mediated adenoviral entry using transferrin control, panels 1, 2, and 3; insets show co-localization in the merged image between clathrin (*green*) and Cy3-HAdV-D37 (*red*), between transferrin (*green*) and Cy3-HAdV-D37 (*red*), and between clathrin (*green*) and transferrin (*red*) respectively, at 1 hpi.

formation, respectively.⁵⁸ In THE cells, both cytochalasin D and B reduced E1A mRNA expression at 2 hpi in a dose-dependent manner (Fig. 6A) ($P \leq 0.05$ for both interventions). It is generally believed that viruses using clathrin-mediated endocytosis enter early endosomes,^{54,59} which then transition to mature endosomes and ultimately fuse into late endosomes/lysosomes.⁵⁷ For adenoviruses, the low pH in late endosomes enables disassembly of the virus protein coat, and facilitates the delivery of genetic material into the nucleus.⁶⁰ Bafilomycin A inhibits vacuolar ATPase,⁶¹ preventing acidification in these endosomes. Pretreatment of THE cells with bafilomycin A did not alter HAdV-D37 E1A mRNA

expression (Fig. 6B), indicating that infection is pH independent.

Macropinocytosis of Adenovirus

Because our TEM data also showed typical macropinosome-like structures in THE cells (Fig. 1E), we investigated macropinocytosis as another possible entry pathway for HAdV-D37.³⁵ Intriguingly, 5-(N-ethyl-N-isopropyl) amiloride, an inhibitor of macropinosome formation⁶² that was previously shown to block uptake of HAdV-B35,⁶³ did not block HAdV-D37 E1A mRNA expression (Fig. 6C). These data

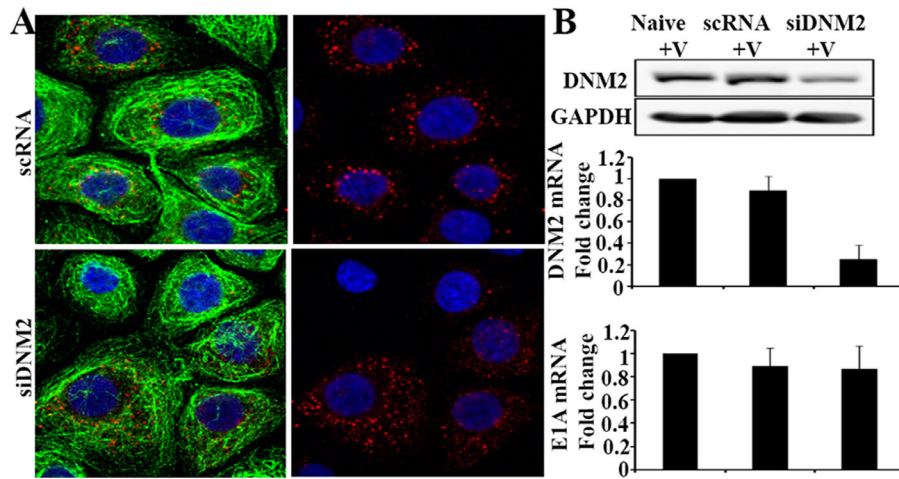


FIGURE 3. Dynamin-independent clathrin-mediated pathway. **(A)** Confocal images reveal no apparent difference in entry of Cy3-HAdV-D37 (*red*) between scRNA (*top*) and dynamin 2 siRNA (siDNM2) treated (*bottom*) THE cells at 2 hpi. Acetylated tubulin staining is shown in green. **(B)** Western blot showing knock down of dynamin 2, along with GAPDH loading control. Successful dynamin 2 knock down was confirmed by RT-qPCR. E1A gene expression at 2 hpi by RT-qPCR showed no difference between control and siDNM2 knock down cells.

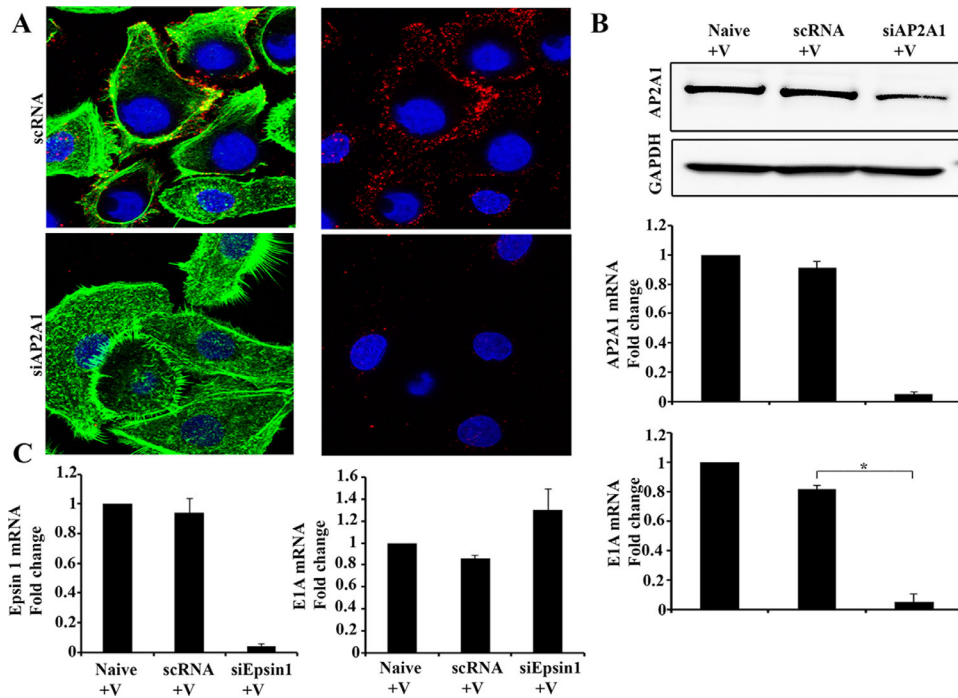


FIGURE 4. AP2A1-dependent, epsin 1-independent pathway. **(A)** Confocal images reveal successful entry of Cy3-HAdV-D37 (*red*) into scRNA treated cells. However, entry was blocked in siAP2A1 treated cells. Phalloidin staining is shown in green. **(B)** Western blot showing AP2A1 knock down, with GAPDH shown as loading control. Bar graphs show mRNA levels after AP2A1 knock down, and near complete abrogation of E1A gene expression in siAP2A1-treated cells ($P \leq 0.05$). **(C)** Epsin1 knock down, as confirmed by RT-qPCR, did not reduce HAdV-D37 E1A gene expression.

may indicate that the macropinosome-like structures seen by TEM may represent membrane ruffling and are not evidence of macropinocytosis. However, macropinocytosis is also regulated downstream by the serine/threonine kinase of p21-activated kinase (Pak).⁶⁴ In THE cells pretreated with the Pak inhibitor IPA-3, E1A mRNA expression was reduced in a dose-dependent manner (Fig. 6D) ($P \leq 0.05$).

Clathrin-Mediated Entry in PHCE Cells

Our biochemical data strongly suggested that HAdV-D37 enters THE cells via a clathrin-mediated pathway. Therefore, we sought to confirm these results in PHCE cells by analysis of the critical components of the clathrin-mediated pathway, including clathrin, AP2A1, and

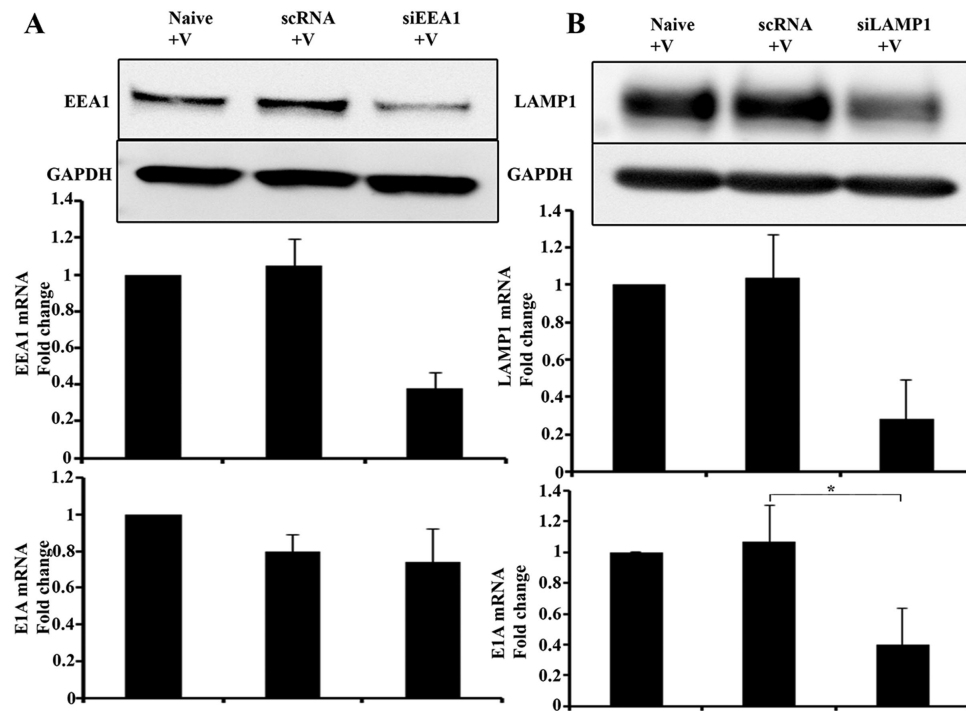


FIGURE 5. HAdV-D37 endosomal trafficking is not canonical. **(A)** EEA1 knock down shown by Western blot, and RT-qPCR (*upper left bar graph*). EIA gene expression was not reduced by siEEA1 pretreatment (*lower left bar graph*). **(B)** LAMP1 knock down shown by Western blot and RT-qPCR (*upper right bar graph*). EIA gene expression was reduced upon siLAMP1 treatment (*lower right bar graph*) ($P \leq 0.05$).

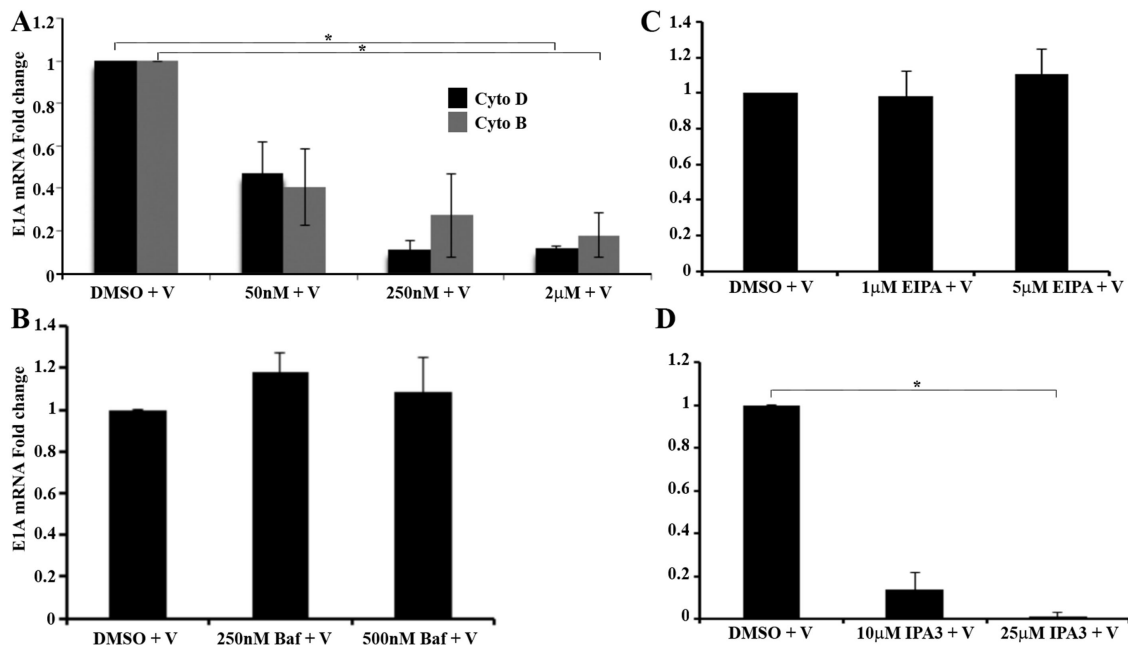


FIGURE 6. Actin is important for HAdV-D37 entry. **(A)** Both cytochalasin inhibitors D and B decreased EIA gene expression in a dose-dependent manner ($P \leq 0.05$). **(B)** Bafilomycin A, an inhibitor of endosome acidification did not reduce EIA gene expression even at high concentration. **(C)** The macropinosome formation inhibitor, EIPA, had no effect on EIA gene expression. **(D)** The Pak1 inhibitor, IPA3, decreased EIA gene expression in a dose-dependent manner ($P \leq 0.05$).

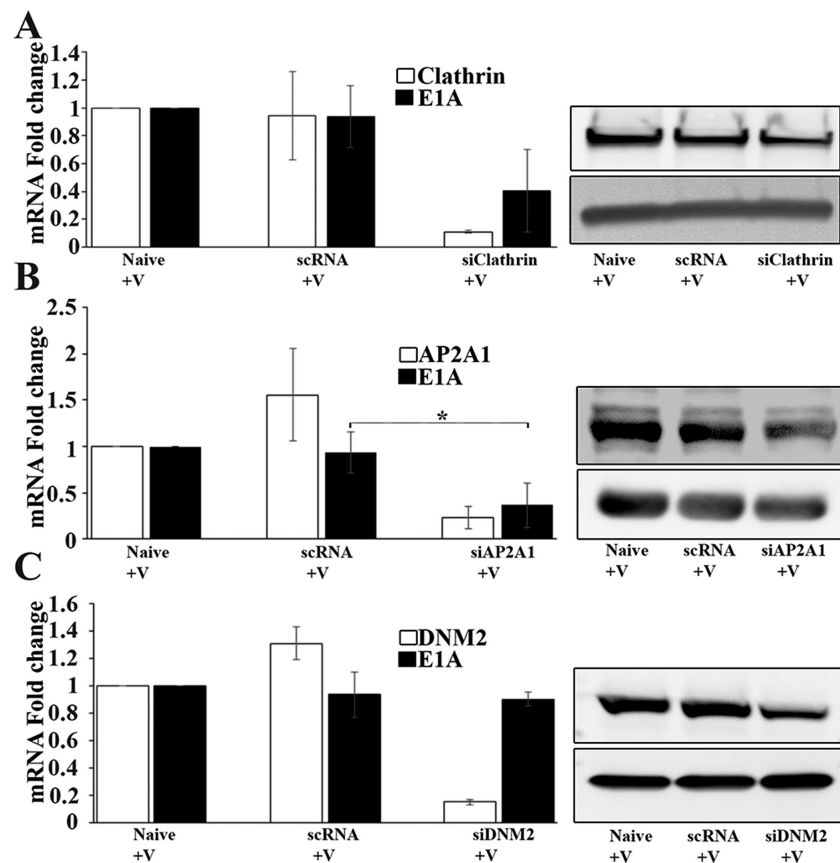


FIGURE 7. Clathrin-mediated entry in PHCE cells. **(A)** *Open bar* shows clathrin mRNA expression; *solid bar* shows E1A mRNA expression. **(B)** Western blot of clathrin and GAPDH load control. **(C)** *Open bar* shows AP2A1 mRNA expression; *solid bar* shows E1A mRNA expression. **(D)** Western blot of AP2A1 and GAPDH load control. **(E)** *Open bar* shows dynamin 2 (DNLM2) mRNA expression; *solid bar* shows E1A mRNA expression. **(F)** Western blot of dynamin 2 and GAPDH load control. * $P = 0.01$, Student *t*-test, comparing E1A mRNA expression between scRNA- and siRNA-treated cells.

dynamin 2. Clathrin knock down by siRNA in PHCE cells, as shown by RT-qPCR (Fig. 7A) and Western blot (Fig. 7B), appeared to decrease subsequent HAdV-D37 E1A gene expression (Fig. 7A), although the result was not statistically significant. AP2A1 is a critical component of the clathrin mediated entry pathway. Knock down of AP2A1 by siRNA treatment, which was shown to reduce both AP2A1 mRNA (Fig. 7C) and protein (Fig. 7D), significantly reduced E1A gene expression in PHCE cells ($P = 0.01$; Fig. 7C). As was observed in THE cells, dynamin 2 siRNA knock down in PHCE cells (Figs. 7E, 7F) did not affect E1A gene expression (Fig. 7E). These results are consistent with entry of HAdV-D37 into human corneal epithelial cells via a clathrin-mediated, dynamin 2-independent pathway.

Caveolin Plays No Role in Adenovirus Entry Into Human Corneal Epithelial Cells

Finally, given our prior work showing that HAdV-D37 enters human keratocytes via a caveolin dependent pathway,²⁵ we wanted investigate if the caveolin pathway is used by human corneal epithelial cells as well. As shown by confocal microscopy with Cy3-labeled HAdV-D37 infection of THE cells, we could not identify colocalization of Cy3 (red) with caveolin 1 (green) (Fig. 8A). In addition, siRNA knock down

of caveolin 1 had no apparent effect on E1A mRNA expression (Fig. 8B).

DISCUSSION

The earliest innate immune responses to viral infection are influenced in large part by the specific route of viral entry and trafficking within infected cells.⁶⁵ Our study of HAdV-D37 entry in keratocytes revealed that viruses trafficking through the cytosol produced less cytokines than viruses that traffic within endosomes.²⁶ We have earlier shown HAdV-D37 enters keratocytes via a caveolin 1 pathway,²⁵ and further showed that dynamin 2 negatively regulates viral entry in these cells.²⁶ Dynamin-dependent and -independent pathways have been demonstrated in entry mechanisms of other viruses.^{66–70} In the current study, because epithelial cells are the first corneal cells to be infected in any ocular surface infection, we investigated viral entry into human corneal epithelial cells. Herein, we show that the EKC agent HAdV-D37 enters human corneal epithelial cells via clathrin coated pits, but with some unique differences from the canonical clathrin-mediated pathway (Fig. 9), and in a dynamin 2-independent manner. We have been unable to detect biologically significant elevations in cytokine expression upon infection of human corneal epithelial cells (manuscript in preparation). However, the potential remains for a feedback relationship between infected epithelial cells

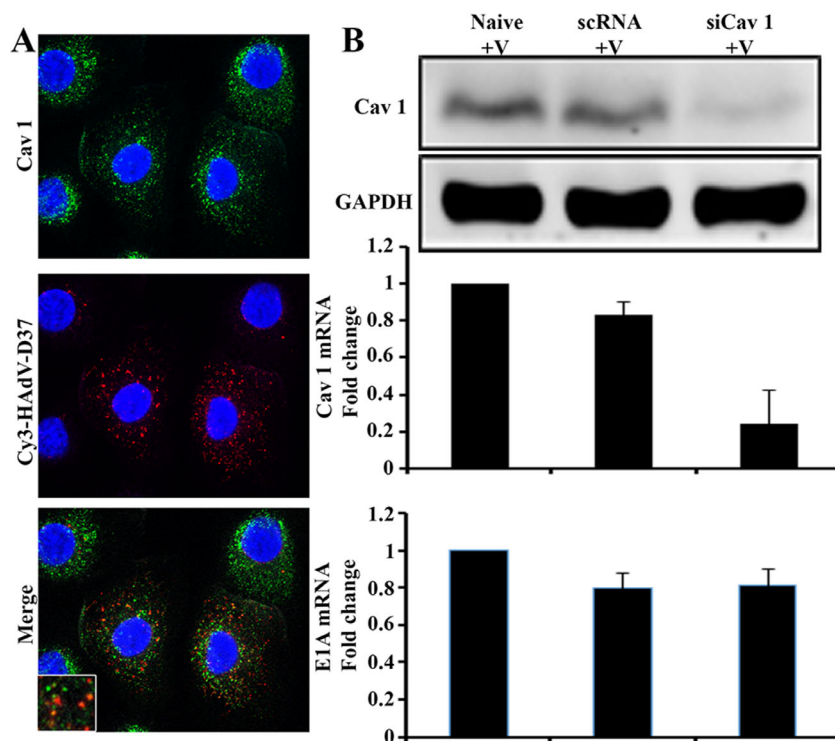


FIGURE 8. HAdV-D37 does not use caveolin to enter human corneal epithelial cells. **(A)** Confocal images in merge tile did not show colocalization of caveolin 1 (green) and Cy3-HAdV-D37 (red). **(B)** Caveolin 1 knock down as shown by Western blot and RT-qPCR (*upper bar graph*) did not decrease E1A gene expression (*lower bar graph*). Experiments were performed at 2 hours after infection.

Viral entry in human corneal epithelial cells

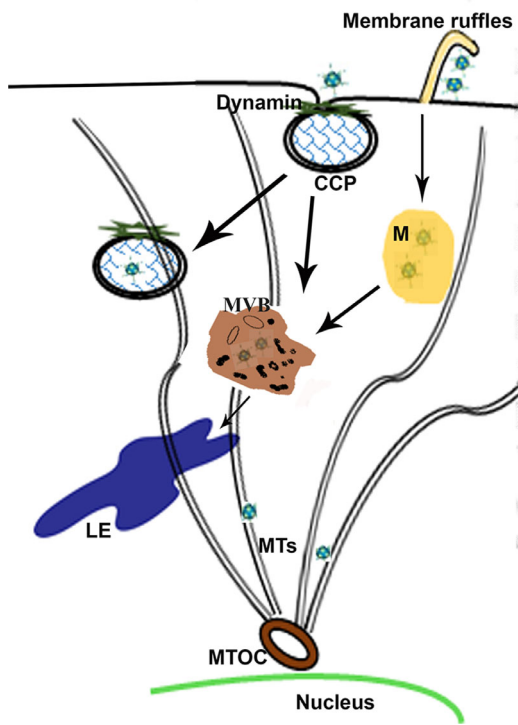


FIGURE 9. Schematic model of HAdV-D37 entry into human corneal epithelial cells. CCP, clathrin-coated pit; MVB, multivesicular body; LE, late endosome; M, macropinosome; MTs, microtubules; MTOC, microtubule organizing center.

and keratocytes during adenoviral infection and deserves further study.

Dogma dictates that, after cell entry, viruses traffic into early endosomes, then to late endosomes, the latter then fuse into lysosomes before viral DNA is delivered into the nucleus. The stepwise nature of this trafficking is understood to be important for uncoating of the viral proteinaceous coat, classically attributed to the low pH in these vesicles. Several proteins are involved in this trafficking paradigm, including EEA1, an effector protein for Rab5 that plays a role in tethering clathrin coated vesicles to early endosomes.⁵⁹ It was previously shown that EEA1 knock down had no effect on HAdV-C2 or -C5 infection,⁵⁹ similar to the data we present herein, suggesting an EEA1 independent entry pathway for adenoviruses. Other key proteins involved in clathrin-mediated endocytosis include actin, epsin, epidermal growth factor receptor pathway substrate clone 15, AP2, dynamin, and the phospholipid phosphatidylinositol 4,5-bisphosphate [PI(4,5)P2], and PI(3,4,5)P3. Clathrin assembles into a polyhedral lattice on the inner side of the plasma membrane to form the coated pit. Epidermal growth factor receptor pathway substrate clone 15 acts as an adaptor between the clathrin coats and AP2.⁷¹ AP2 in turn belongs to a family of heterotetrameric complex proteins, which typically include two large subunits (α and β), one medium size subunit (μ), and a small subunit (σ). These adaptor proteins assist in the assembly of clathrin coated vesicles by interacting with lipids and/or proteins at the plasma membrane.⁷² Although these molecules are important for clathrin pit formation and entry, some are dispensable during endocytosis. AP2A1 subunit knock down decreased entry of human enterovirus 71 by 60% in human rhabdomyosarcoma cells,⁷³ but a role

for the adaptor protein complex in adenoviral entry has never been studied. Here, we show that knock down of AP2A1 completely abolished HAdV-D37 entry into human corneal epithelial cells. Epsin 1, a critical secondary adaptor molecule in clathrin-coated pits, was shown to be important in the internalization of influenza virus.⁵² However, AP2-dependent, epsin 1-independent endocytosis has been previously reported.⁷⁴ In corneal epithelial cells infected with HAdV-D37, viral entry was similarly AP2 dependent and epsin 1 independent.

Although these results confirmed a clathrin-mediated entry pathway for adenoviruses in human corneal epithelial cells, intriguingly, our results indicated that the entry was not pH dependent. The vacuolar-H⁺ ATPase is a proton pump consisting of a multi-subunit membrane protein. This proton pump controls the acidification of endosomes, lysosomes, and other vesicles including Golgi-derived secretory vesicles.⁷⁵ Pretreatment with bafilomycin A, known to inhibit the vacuolar-H⁺ ATPase and prevent acidification of these vacuoles, did not alter adenoviral gene expression. These data indicate that an acidic pH is unnecessary for successful HAdV-D37 trafficking to the nucleus of human corneal epithelial cells. Enterovirus B was also shown to traffic by multivesicular body-containing endosomes with neutral pH.⁷⁶ However, how these viruses uncoat in the absence of low pH is still not understood.

In human corneal epithelial cells infected with HAdV-D37, transmission electron microscopy showed association of adenovirions with both clathrin coated pits and membrane ruffles, the latter suggestive of micropinocytosis. Testing with the macropinocytosis inhibitor EIPA did not show an effect on adenoviral gene expression. However, it is possible, that upon inhibition of macropinocytosis, a compensatory increase in clathrin-mediated entry may have occurred, explaining the null effect of EIPA on viral gene expression. Blocking the downstream signaling of p21-activated kinase 1 (Pak1) using IPA3 did indeed reduce viral gene expression. Pak1 has been shown to play an important role in signaling pathways associated with cytoskeletal modifications and filopodia formation,^{77,78} and therefore cell motility.⁷⁹ Hence, data showing that both IPA3 and cytochalasins D and B inhibited viral trafficking suggests that the actin cytoskeleton plays a major role in HAdV-D37 entry, and may indicate a secondary role for macropinocytosis in adenoviral entry in corneal epithelial cells. Caveolin-mediated entry was shown earlier to be the sole pathway for HAdV-D37 entry in human keratocytes,²⁵ but we found no evidence of a role for caveolin in entry of HAdV-D37 in corneal epithelial cells.

Finally, although we saw similar results in both primary and immortalized human corneal epithelial cells, one observation worth noting was that, in primary epithelial cells, cell membrane ruffling upon virus infection appeared more distinct. Also, for experiments in primary cells, we used pooled cultures; this process was necessary to have sufficient cells for each experiment. If sex of the donor has an effect on viral entry pathway, the use of pooled cells might have obscured any differences.

In summary, the data presented here strongly suggest that HAdV-D37 enters corneal epithelial cells via a noncanonical, clathrin-mediated pathway, not dependent on dynamin 2 or early endosomes.

Acknowledgments

The authors gratefully thank Maria Ericsson at the Conventional Electron Microscopy Facility, Harvard Medical School, for technical assistance.

Supported by National Institutes of Health grants EY013124, EY021558, and EY014104, an unrestricted grant to the Department of Ophthalmology, Harvard Medical School from Research to Prevent Blindness, Inc., New York, New York; The Falk Foundation; and the Massachusetts Lions Eye Research Fund.

Disclosure: **J.S. Lee**, None; **S. Mukherjee**, None; **J.Y. Lee**, None; **A. Saha**, None; **J. Chodosh**, Santen, US Food & Drug Administration; **D.F. Painter**, None; **J. Rajaiya**, None

References

1. Lion T. Adenovirus infections in immunocompetent and immunocompromised patients. *Clin Microbiol Rev.* 2014;27:441–462.
2. Robinson CM, Singh G, Lee JY, et al. Molecular evolution of human adenoviruses. *Sci Rep.* 2013;3:1812.
3. Ford E, Nelson KE, Warren D. Epidemiology of epidemic keratoconjunctivitis. *Epidemiol Rev.* 1987;9:244–261.
4. Zhou X, Robinson CM, Rajaiya J, et al. Analysis of human adenovirus type 19 associated with epidemic keratoconjunctivitis and its reclassification as adenovirus type 64. *Invest Ophthalmol Vis Sci.* 2012;53:2804–2811.
5. Jhanji V, Chan TC, Li EY, Agarwal K, Vajpayee RB. Adenoviral keratoconjunctivitis. *Surv Ophthalmol.* 2015;60:435–443.
6. Chandra N, Frangsmyr L, Arnberg N. Decoy receptor interactions as novel drug targets against EKC-causing human adenovirus. *Viruses.* 2019;11:242.
7. Stichling N, Suomalainen M, Flatt JW, et al. Lung macrophage scavenger receptor SR-A6 (MARCO) is an adenovirus type-specific virus entry receptor. *PLoS Pathog.* 2018;14:e1006914.
8. Suomalainen M, Nakano MY, Boucke K, Keller S, Greber UF. Adenovirus-activated PKA and p38/MAPK pathways boost microtubule-mediated nuclear targeting of virus. *EMBO J.* 2001;20:1310–1319.
9. Wolfrum N, Greber UF. Adenovirus signalling in entry. *Cell Microbiol.* 2013;15:53–62.
10. Greber UF, Flatt JW. Adenovirus entry: from infection to immunity. *Annu Rev Virol.* 2019;6:177–197.
11. Iacobelli-Martinez M, Nemerow GR. Preferential activation of Toll-like receptor nine by CD46-utilizing adenoviruses. *J Virol.* 2007;81:1305–1312.
12. Roelvink PW, Lizonova A, Lee JG, et al. The coxsackievirus-adenovirus receptor protein can function as a cellular attachment protein for adenovirus serotypes from subgroups A, C, D, E, and F. *J Virol.* 1998;72:7909–7915.
13. Nilsson EC, Storm RJ, Bauer J, et al. The GD1a glycan is a cellular receptor for adenoviruses causing epidemic keratoconjunctivitis. *Nat Med.* 2011;17:105–109.
14. Caraballo R, Saleeb M, Bauer J, et al. Triazole linker-based trivalent sialic acid inhibitors of adenovirus type 37 infection of human corneal epithelial cells. *Org Biomol Chem.* 2015;13:9194–9205.
15. Chandra N, Frangsmyr L, Imhof S, Caraballo R, Elofsson M, Arnberg N. Sialic acid-containing glycans as cellular receptors for ocular human adenoviruses: implications for tropism and treatment. *Viruses.* 2019;11:395.
16. Chandra N, Liu Y, Liu JX, et al. Sulfated glycosaminoglycans as viral decoy receptors for human adenovirus type 37. *Viruses.* 2019;11:247.

17. Mathias P, Wickham T, Moore M, Nemerow G. Multiple adenovirus serotypes use alpha v integrins for infection. *J Virol.* 1994;68:6811–6814.
18. Wickham TJ, Mathias P, Cheresh DA, Nemerow GR. Integrins alpha v beta 3 and alpha v beta 5 promote adenovirus internalization but not virus attachment. *Cell.* 1993;73:309–319.
19. Bruder JT, Kovesdi I. Adenovirus infection stimulates the Raf/MAPK signaling pathway and induces interleukin-8 expression. *J Virol.* 1997;71:398–404.
20. Mercer J, Schelhaas M, Helenius A. Virus entry by endocytosis. *Annu Rev Biochem.* 2010;79:803–833.
21. Chardonnet Y, Dales S. Early events in the interaction of adenoviruses with HeLa cells. I. Penetration of type 5 and intracellular release of the DNA genome. *Virology.* 1970;40:462–477.
22. FitzGerald DJ, Padmanabhan R, Pastan I, Willingham MC. Adenovirus-induced release of epidermal growth factor and pseudomonas toxin into the cytosol of KB cells during receptor-mediated endocytosis. *Cell.* 1983;32:607–617.
23. Xie J, Chiang L, Contreras J, et al. Novel fiber-dependent entry mechanism for adenovirus serotype 5 in lacrimal acini. *J Virol.* 2006;80:11833–11851.
24. Amstutz B, Gastaldelli M, Kalin S, et al. Subversion of CtBP1-controlled macropinocytosis by human adenovirus serotype 3. *EMBO J.* 2008;27:956–969.
25. Yousuf MA, Zhou X, Mukherjee S, et al. Caveolin-1 associated adenovirus entry into human corneal cells. *PLoS One.* 2013;8:e77462.
26. Lee JS, Ismail AM, Lee JY, et al. Impact of dynamin 2 on adenovirus nuclear entry. *Virology.* 2019;529:43–56.
27. Pennington MR, Saha A, Painter DF, et al. Disparate entry of adenoviruses dictates differential innate immune responses on the ocular surface. *Microorganisms.* 2019;7:351.
28. Oakes JE, Monteiro CA, Cubitt CL, Lausch RN. Induction of interleukin-8 gene expression is associated with herpes simplex virus infection of human corneal keratocytes but not human corneal epithelial cells. *J Virol.* 1993;67:4777–4784.
29. de Jong JC, Wigand R, Wadell G, et al. Adenovirus 37: identification and characterization of a medically important new adenovirus type of subgroup D. *J Med Virol.* 1981;7:105–118.
30. Robinson CM, Shariati F, Gillaspay AF, Dyer DW, Chodosh J. Genomic and bioinformatics analysis of human adenovirus type 37: new insights into corneal tropism. *BMC Genomics.* 2008;9:213.
31. Leopold PL, Ferris B, Grinberg I, Worgall S, Hackett NR, Crystal RG. Fluorescent virions: dynamic tracking of the pathway of adenoviral gene transfer vectors in living cells. *Hum Gene Ther.* 1998;9:367–378.
32. de Vries E, Tscherne DM, Wienholts MJ, et al. Dissection of the influenza A virus endocytic routes reveals macropinocytosis as an alternative entry pathway. *PLoS Pathog.* 2011;7:e1001329.
33. Meier O, Boucke K, Hammer SV, et al. Adenovirus triggers macropinocytosis and endosomal leakage together with its clathrin-mediated uptake. *J Cell Biol.* 2002;158:1119–1131.
34. Robertson DM, Li L, Fisher S, et al. Characterization of growth and differentiation in a telomerase-immortalized human corneal epithelial cell line. *Invest Ophthalmol Vis Sci.* 2005;46:470–478.
35. Stahl PD, Barbieri MA. Multivesicular bodies and multivesicular endosomes: the "ins and outs" of endosomal traffic. *Sci STKE.* 2002;2002:pe32.
36. Fader CM, Colombo MI. Autophagy and multivesicular bodies: two closely related partners. *Cell Death Differ.* 2009;16:70–78.
37. Dobrowolski R, De Robertis EM. Endocytic control of growth factor signalling: multivesicular bodies as signalling organelles. *Nat Rev Mol Cell Biol.* 2011;13:53–60.
38. Suomalainen M, Luisoni S, Boucke K, Bianchi S, Engel DA, Greber UF. A direct and versatile assay measuring membrane penetration of adenovirus in single cells. *J Virol.* 2013;87:12367–12379.
39. Salinas S, Zussy C, Loustalot F, et al. Disruption of the coxsackievirus and adenovirus receptor-homodimeric interaction triggers lipid microdomain- and dynamin-dependent endocytosis and lysosomal targeting. *J Biol Chem.* 2014;289:680–695.
40. Carvajal-Gonzalez JM, Gravotta D, Mattera R, et al. Basolateral sorting of the coxsackie and adenovirus receptor through interaction of a canonical YXXPhi motif with the clathrin adaptors AP-1A and AP-1B. *Proc Natl Acad Sci USA.* 2012;109:3820–3825.
41. Delos Santos RC, Bautista S, Lucarelli S, et al. Selective regulation of clathrin-mediated epidermal growth factor receptor signaling and endocytosis by phospholipase C and calcium. *Mol Biol Cell.* 2017;28:2802–2818.
42. Kim JH, Singh A, Del Poeta M, Brown DA, London E. The effect of sterol structure upon clathrin-mediated and clathrin-independent endocytosis. *J Cell Sci.* 2017;130:2682–2695.
43. He Q, Bouley R, Liu Z, et al. Large G protein alpha-subunit XLalphas limits clathrin-mediated endocytosis and regulates tissue iron levels in vivo. *Proc Natl Acad Sci USA.* 2017;114:E9559–E9568.
44. Tanabe K, Takei K. Dynamic instability of microtubules requires dynamin 2 and is impaired in a Charcot-Marie-Tooth mutant. *J Cell Biol.* 2009;185:939–948.
45. Henley JR, Cao H, McNiven MA. Participation of dynamin in the biogenesis of cytoplasmic vesicles. *FASEB J.* 1999;13(Suppl 2):S243–247.
46. Scherer J, Vallee RB. Adenovirus recruits dynein by an evolutionary novel mechanism involving direct binding to pH-primed hexon. *Viruses.* 2011;3:1417–1431.
47. Johannessen LE, Pedersen NM, Pedersen KW, Madshus IH, Stang E. Activation of the epidermal growth factor (EGF) receptor induces formation of EGF receptor- and Grb2-containing clathrin-coated pits. *Mol Cell Biol.* 2006;26:389–401.
48. Maurer ME, Cooper JA. The adaptor protein Dab2 sorts LDL receptors into coated pits independently of AP-2 and ARH. *J Cell Sci.* 2006;119:4235–4246.
49. Huang F, Khvorova A, Marshall W, Sorkin A. Analysis of clathrin-mediated endocytosis of epidermal growth factor receptor by RNA interference. *J Biol Chem.* 2004;279:16657–16661.
50. Motley A, Bright NA, Seaman MN, Robinson MS. Clathrin-mediated endocytosis in AP-2-depleted cells. *J Cell Biol.* 2003;162:909–918.
51. Loerke D, Mettlen M, Yarar D, et al. Cargo and dynamin regulate clathrin-coated pit maturation. *PLoS Biol.* 2009;7:e57.
52. Chen C, Zhuang X. Epsin 1 is a cargo-specific adaptor for the clathrin-mediated endocytosis of the influenza virus. *Proc Natl Acad Sci USA.* 2008;105:11790–11795.
53. Zerial M, McBride H. Rab proteins as membrane organizers. *Nat Rev Mol Cell Biol.* 2001;2:107–117.
54. Simonsen A, Lippe R, Christoforidis S, et al. EEA1 links PI(3)K function to Rab5 regulation of endosome fusion. *Nature.* 1998;394:494–498.
55. Stradal TEB, Schelhaas M. Actin dynamics in host-pathogen interaction. *FEBS Lett.* 2018;592:3658–3669.

56. Taylor MP, Koyuncu OO, Enquist LW. Subversion of the actin cytoskeleton during viral infection. *Nat Rev Microbiol.* 2011;9:427–439.
57. Mooren OL, Galletta BJ, Cooper JA. Roles for actin assembly in endocytosis. *Annu Rev Biochem.* 2012;81:661–686.
58. Cooper JA. Effects of cytochalasin and phalloidin on actin. *J Cell Biol.* 1987;105:1473–1478.
59. Gastaldelli M, Imelli N, Boucke K, Amstutz B, Meier O, Greber UF. Infectious adenovirus type 2 transport through early but not late endosomes. *Traffic.* 2008;9:2265–2278.
60. Prchla E, Kuechler E, Blaas D, Fuchs R. Uncoating of human rhinovirus serotype 2 from late endosomes. *J Virol.* 1994;68:3713–3723.
61. Gagliardi S, Rees M, Farina C. Chemistry and structure activity relationships of bafilomycin A1, a potent and selective inhibitor of the vacuolar H⁺-ATPase. *Curr Med Chem.* 1999;6:1197–1212.
62. Swanson JA, Watts C. Macropinocytosis. *Trends Cell Biol.* 1995;5:424–428.
63. Kalin S, Amstutz B, Gastaldelli M, et al. Macropinocytotic uptake and infection of human epithelial cells with species B2 adenovirus type 35. *J Virol.* 2010;84:5336–5350.
64. Dharmawardhane S, Schurmann A, Sells MA, Chernoff J, Schmid SL, Bokoch GM. Regulation of macropinocytosis by p21-activated kinase-1. *Mol Biol Cell.* 2000;11:3341–3352.
65. Teigler JE, Kagan JC, Barouch DH. Late endosomal trafficking of alternative serotype adenovirus vaccine vectors augments antiviral innate immunity. *J Virol.* 2014;88:10354–10363.
66. Mockel M, Rahn E, de la Cruz N, et al. Herpes Simplex Virus 1 Can Enter Dynamin 1 and 2 Double-Knockout Fibroblasts. *J Virol.* 2019;93:e00704.
67. Rahn E, Petermann P, Hsu MJ, Rixon FJ, Knebel-Morsdorf D. Entry pathways of herpes simplex virus type 1 into human keratinocytes are dynamin- and cholesterol-dependent. *PLoS One.* 2011;6:e25464.
68. Mettlen M, Pucadyil T, Ramachandran R, Schmid SL. Dissecting dynamin's role in clathrin-mediated endocytosis. *Biochem Soc Trans.* 2009;37:1022–1026.
69. Mues MB, Cheshenko N, Wilson DW, Gunther-Cummins L, Herold BC. Dynasore disrupts trafficking of herpes simplex virus proteins. *J Virol.* 2015;89:6673–6684.
70. Gianni T, Gatta V, Campadelli-Fiume G. α V β 3-integrin routes herpes simplex virus to an entry pathway dependent on cholesterol-rich lipid rafts and dynamin2. *Proc Natl Acad Sci USA.* 2010;107:22260–22265.
71. Doherty GJ, McMahon HT. Mechanisms of endocytosis. *Annu Rev Biochem.* 2009;78:857–902.
72. Maldonado-Baez L, Wendland B. Endocytic adaptors: recruiters, coordinators and regulators. *Trends Cell Biol.* 2006;16:505–513.
73. Hussain KM, Leong KL, Ng MM, Chu JJ. The essential role of clathrin-mediated endocytosis in the infectious entry of human enterovirus 71. *J Biol Chem.* 2011;286:309–321.
74. Deinhardt K, Berninghausen O, Willison HJ, Hopkins CR, Schiavo G. Tetanus toxin is internalized by a sequential clathrin-dependent mechanism initiated within lipid microdomains and independent of epsin1. *J Cell Biol.* 2006;174:459–471.
75. Forgac M. Vacuolar ATPases: rotary proton pumps in physiology and pathophysiology. *Nat Rev Mol Cell Biol.* 2007;8:917–929.
76. Marjomaki V, Turkki P, Huttunen M. Infectious entry pathway of enterovirus B species. *Viruses.* 2015;7:6387–6399.
77. Itakura A, Aslan JE, Kusanto BT, et al. p21-Activated kinase (PAK) regulates cytoskeletal reorganization and directional migration in human neutrophils. *PLoS One.* 2013;8:e73063.
78. Abo A, Qu J, Cammarano MS, et al. PAK4, a novel effector for Cdc42Hs, is implicated in the reorganization of the actin cytoskeleton and in the formation of filopodia. *EMBO J.* 1998;17:6527–6540.
79. Sells MA, Boyd JT, Chernoff J. p21-activated kinase 1 (Pak1) regulates cell motility in mammalian fibroblasts. *J Cell Biol.* 1999;145:837–849.